Pulsatile Blood Flows Through a Bileaflet Mechanical Heart Valve with Different Approach Methods of Numerical Analysis ; Pulsatile Flows with Fixed Leaflets and Interacted with Moving Leaflets

Choeng Ryul Choi
Mechanical Engineering Department, Graduate School of Kyunghee University, 1 Seochon, Kihung, Yongin, Kyunggi 449-701, Korea
Chang Nyung Kim*
College of Mechanical & Industrial System Engineering, Kyunghee University, 1 Seochon, Kihung, Yongin, Kyunggi 449-701, Korea
Young Joo Kwon
Department of Mechano-Informatics & Design Engineering, Hongik University, Chochiwon, Yeonki-kun, choongnam 339-701, Korea
Jae Won Lee
Department of Thoracic & Cardiovascular Surgery, Asan Medical Center, Ulsan University, San 29, Muger 2-dong, Namgu, Ulsan 680-749, Korea

Many researchers have investigated the blood flow characteristics through bileaflet mechanical heart valves using computational fluid dynamics (CFD) models. Their numerical approach methods can be classified into three types; steady flow analysis, pulsatile flow analysis with fixed leaflets, and pulsatile flow analysis with moving leaflets. The first and second methods have been generally employed for two-dimensional and three-dimensional calculations. The pulsatile flow analysis interacted with moving leaflets has been recently introduced and tried only in two-dimensional analysis because this approach method has difficulty in considering simultaneously two physics of blood flow and leaflet behavior interacted with blood flow. In this publication, numerical calculation for pulsatile flow with moving leaflets using a fluid-structure interaction method has been performed in a three-dimensional geometry. Also, pulsatile flow with fixed leaflets has been analyzed for comparison with the case with moving leaflets. The calculated results using the fluid-structure interaction model have shown good agreements with results visualized by previous experiments. In peak systole, calculations with the two approach methods have predicted similar flow fields. However, the model with fixed leaflets has not been able to predict the flow fields during opening and closing phases. Therefore, the model with moving leaflets is rigorously required for advanced analysis of flow fields.

Key Words : Computational Fluid Dynamics (CFD), Fluid-Structure Interaction (FSI), Mechanical Heart Valve (MHV), Pulsatile Flow

Nomenclature

$[C]$: Damping matrix
$\{F\}$: Force vector
IC : Influence coefficient
J : Coordinate transformation Jacobian.
$[K]$: Stiffness matrix
$[M]$: Mass matrix
$\{p\}_b$: Pressure at fluid-structure boundary
q : Displacement vector

* Corresponding Author,
E-mail : cnkim@khu.ac.kr
TEL : +82-31-202-9715; **FAX** : +82-31-202-8106
College of Mechanical & Industrial System Engineering, Kyunghee University, 1 Seochon, Kihung, Yongin, Kyunggi 449-701, Korea. (Manuscript **Received** November 23, 2002; **Revised** April 18, 2003)

$\{\dot{q}\}_b$: Velocity of structure at fluid-structure interface
t : Time
u_i : Cartesian velocity component
J_j : Velocity component
x_i : Cartesian coordinate

Greek Letters

ρ : Density
μ : Kinetic viscosity
θ : Leaflet angle
τ : Shear stress

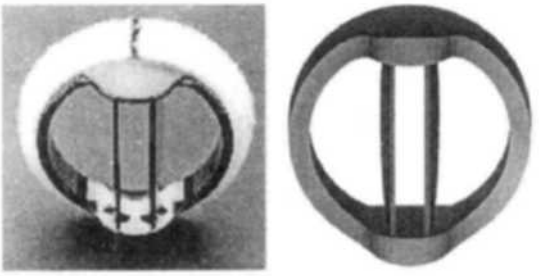

Fig. 1 Photograph and 3D model reconstructed for a bileaflet mechanical heart valve (St. Jude medical)

1. Introduction

A heart of human consists of two atria and two ventricles, and has four heart valves to allow forward flow and to prevent backward flow of blood. Healthy valve leaflets are formed thin and pliable tissues that open and close as heart contracts and relaxes. However, heart valves can be abnormally formed congenitally. Also they can be damaged or scarred by rheumatic fever, infection, inherited conditions, aging and heart attacks. In some cases it is possible to repair a valve by performing a surgical procedure called valvotomy, valvuloplasty, or heart valve repair. Although if a heart valve is so seriously deformed or diseased, it must be removed and replaced with a prosthetic heart valve. There are two main types of prosthetic heart valves ; bioprostheses and mechanical heart valves. Bioprostheses or bioprosthetic heart valves are made of biological tissue (human or treated animal tissues). Mechanical heart valves are made of metal, carbon, and/or synthetics. Bileaflet mechanical heart valves (MHV) are the most commonly implanted prosthetic heart valves (Fig. 1). Although these valves function adequately, they require constant anticoagulation therapy to prevent thrombosis and thromboembolism.

Several features of the valve and the flow fields associated with the valve are known to increase the probability of blood clots formation. As the leaflet edge approaches the housing, blood is squeezed out through small gaps between leaflets resulting strong jets (Bluestein et al., 1994 ; Cape et al., 1990). These jets cause higher shear stresses, which may cause red blood cell damage and platelet activation. Area of stasis or slow moving fluid may lead to clot formation. As the valve opens, the valve leaflets act as an obstruction to the blood flow through valve, and three high velocity jets can be readily detected downstream of the valve by both in vivo and in vitro experiments. Instability in the flow downstream of the valve and at the edge of these jets causes high velocity gradients and high shear stresses, which may causes platelet activation or red blood cell damage (Chandran, 1985 ; Fatermi et al., 1989 ; Gross et al., 1988 ; Hasenkam et al., 1988 ; Nygaard et al., 1994 ; Woo et al., 1986).

An improvement of valve design requires a detailed understanding of these system properties and demands further substantial research. Most of researches have been performed through in vitro experimental studies since in vivo experimental investigations are extremely difficult. Although many important aspects of hemodynamic blood flow have been investigated in experimental studies (see the literature cited in Krafczyk et al., 2001b), these studies sometimes lack spatial resolution, have problems analyzing transient phenomena or partially lack the detailed observation of theoretically interesting variables crucial for extended modeling.

Analysis of computational fluid dynamics (CFD) is an alternative tool that can be used to investigate complex flow patterns within the valve and downstream of heart valves. Once a CFD model is defined and validated, small changes can

be made to one design parameter, such as the leaflet-opening angle, and the effect of this alteration on the flow field can be thoroughly investigated.

In the field of numerical analysis, several works can be found in the technical literature investigating steady flow of blood (Krafczyk et al., 2001b). Most of simulations described in the literature have used FEM, FV or FD schemes to discretize the equations under investigation, usually the Navier-Stokes equation coupled with a continuity equation. In a recent work of Krafczyk et al. (1998a), they have analyzed a transient (pulsatile) three-dimensional flow with fixed leaflets. Ideally one would like to analyze a fully transient three-dimensional model including moving leaflets. Also Krafczyk et al. (2001b) have performed a two-dimensional simulation of fluid-structure interaction using the lattice-Boltzmann methods. Choi et al. (2001a, 2001b) have calculated a transient two-dimensional flow through MHV with different maximum opening angles including moving leaflets. Previous numerical approach methods can be classified into three types; steady flow analysis, pulsatile flow analysis with fixed leaflets, and pulsatile flow analysis with moving leaflets.

In this publication, numerical approach method considering fluid-structure interaction between blood flow and leaflet behavior is introduced. In this approach, a finite volume computational fluid dynamics code and a finite element structural dynamics code are used concurrently to solve the flow and structure equations, respectively, where the two equations are strongly coupled.

A transient three-dimensional flow analysis interacted with moving leaflets is performed firstly, and a valve leaflet motion is calculated with time. The evolving velocity patterns and shear stresses of blood flow passing through the MHV are calculated and discussed. Also, a calculation for transient three-dimensional flow with fixed leaflets is performed under the identical flow conditions to that of the case with the moving leaflets. The results of the two cases have been compared. To our knowledge the present study is the first attempt for three-dimensional analysis considering the fluid-structure interaction of moving leaflets driven by a physiological blood flow during a complete heart beat cycle. A fluid-structure interaction model introduced in this paper can be extended to various problems where motions of fluid and structure are correlated.

2. Mathematical Model

The governing equations for fluid dynamics and structural dynamics are considered simultaneously. The moving grid capability is used to account for the change in a flow domain configuration associated with valve motion.

2.1 Governing equations for blood flow

Blood flow has been modeled as pulsatile, laminar, incompressible, and Newtonian flow. The governing equations for blood flow are the continuity equation and the Navier-Stokes equation, which can be written in a strong conservation form in the curvilinear coordinates as follows;

$$\frac{\partial}{\partial t}\left(\frac{\rho}{J}\right)+\frac{\partial}{\partial \xi^j}\left(\frac{\rho U_j}{J}\right)=0 \tag{1}$$

$$\frac{\partial}{\partial t}\left(\frac{\rho u_i}{J}\right)+\frac{\partial}{\partial \xi^j}\left(\frac{\partial U_j u_i}{J}\right)=-\frac{1}{J}\frac{\partial \xi^j}{\partial x_i}\frac{\partial p}{\partial \xi^j}+\frac{\partial}{\partial \xi^k}\left[\frac{\mu}{J}\frac{\partial \xi^k}{\partial x_j}\left(\frac{\partial \xi^l}{\partial x_j}\frac{\partial u_i}{\partial \xi^l}+\frac{\partial \xi^l}{\partial x_i}\frac{\partial u_j}{\partial \xi^l}-\frac{2}{3}\delta_{ij}\frac{\partial u_l}{\partial \xi^m}\frac{\partial \xi^m}{\partial x_l}\right)\right] \tag{2}$$

where u_i is the Cartesian velocity component, x_i the Cartesian coordinate, U_j the velocity component in the ξ^j direction (contravariant velocity component), and J is the coordinate transformation Jacobian.

$$x_1=x,\ x_2=y,\ x_3=z,\ \xi^1=\xi,\ \xi^2=\eta,\ \xi^3=\zeta \tag{3}$$

$$U_j=\frac{\partial \xi^j}{\partial t}+\frac{\partial \xi^j}{\partial x_i}u_i=0 \tag{4}$$

where $\frac{\partial \xi^j}{\partial t}$ represents the grid velocity, so that the above formulation is in an Eulerian-Lagrangian frame.

2.2 Governing equations for structural dynamics

The finite element formulation of the structural

dynamics equation can be generally written in a linear form as follows;

$$[M]\{\ddot{q}\}+[C]\{\dot{q}\}+[K]\{q\}=\{F\} \quad (5)$$

where $\{q\}$ is the displacement vector, $[M]$ the mass matrix, $[C]$ the damping matrix, $[K]$ the stiffness matrix, and $\{F\}$ the force vector caused by the fluid dynamic load and shear stresses.

The Newmark's scheme is applied to solve Eq. (5). For known values of q, $\dot{q}$, $\ddot{q}$ at (n-1)th time step, we have

$$\{\dot{q}\}=\frac{2}{\Delta t}\left[[K]+\frac{4}{\Delta t^2}[M]+\frac{2}{\Delta t}[C]\right]^{-1}\{F\}+\{E\} \quad (6)$$

where $\{E\}$ comprises all the terms of q^{n-1}, $\dot{q}^{n-1}$ and $\ddot{q}^{n-1}$.

2.3 Coupling of fluid and structure

In Eq. (2) of fluid dynamics, the structural effect comes into play only through the grid velocity term. This section will discuss the implicit coupling procedure. It is known that at the fluid-structure interface fluid velocity is always equal to the structure velocity and the contravariant velocity component in the Eulerian-Lagrangian formulation is zero as shown in Eq. (4).

If $\{\dot{q}\}_b$ is the velocity of structure at the fluid-structure interface, then

$$\{\dot{q}\}_b=-\frac{\partial \xi^j}{\partial t}=\frac{\partial \xi^j}{\partial x_i}u_i \quad (7)$$

On the other hand, Eq. (6) can be simplified in the following perturbation form by introducing the influence coefficient, $[IC]$.

$$\{\dot{q}\}'_b=[IC]\{p\}'_b \quad (8)$$

In view of Eq. (6), we have

$$\frac{\partial \xi^j}{\partial x_i}u'_i=[IC]\{p\}'_b \quad (9)$$

where $[IC]$ and $\{p\}_b$ are the influence coefficient (Yang et al., 1994) and the pressure at the fluid-structure interface, respectively. When Eq. (9) is substituted into the pressure gradient term of the pressure correction equation, the resulting equation depends only on flow variables.

In the process of numerical calculation fluid velocities and pressures are computed at each time step solving the Navier-Stokes momentum and continuity equations. The fluid and structural dynamics models and the fluid-structure interaction method are embedded in the iterative procedure. In the process of fluid-structure interaction, fluid forces on the valve during each iteration are used to compute leaflet motion. On the contrary, the leaflet surface velocity is imposed on the fluid in the altered flow domain during the next iteration, which means that the fluid-structure interface is moving. Fluid velocities and pressures are once again computed and the updated fluid forces on the leaflet are applied as boundary conditions of the structure (leaflet). This process continues until both the flow variables and structural behavior converge to equilibrium values. The numerical computation then proceeds to the next time step and the entire procedure is repeated. The rigorous scheme ensures fully coupled flow and structural solutions at each time step. A time accurate, backward Euler, upwind differencing SIMPLEC scheme has been used in the flow solver.

3. Calculation Process

Calculations were performed to the flow passing through MHV installed in the position of aorta. Firstly, a transient three-dimensional flow interacted with leaflet motion (case 1) was calculated. Then, a transient three-dimensional flow with fixed leaflets (case 2) was simulated using the flow condition resulting from case 1.

The geometry of the simulated flow problems is shown in Fig. 2. The geometry of sinuses and downstream region were based on the published data by Reul et al. (1990). Currently implanted valve was modeled from a 27 mm aortic valve of St. Jude medical. For case 1, leaflet opening angle is varying between $25°\leq\theta\leq85°$ with pulsatile flow of blood related with contractions and relaxes of heart. The leaflet opening angle is calculated in the each time step by the fluid-structure interaction method. For the case 2, Leaflet opening angle was assumed as a fixed angles of $\theta=85°$. Blood was modeled as Newtonian fluid. Density is 1,000 kg/m^3 and dynamic viscosity is 3.5×10^{-3} kg/m·s.

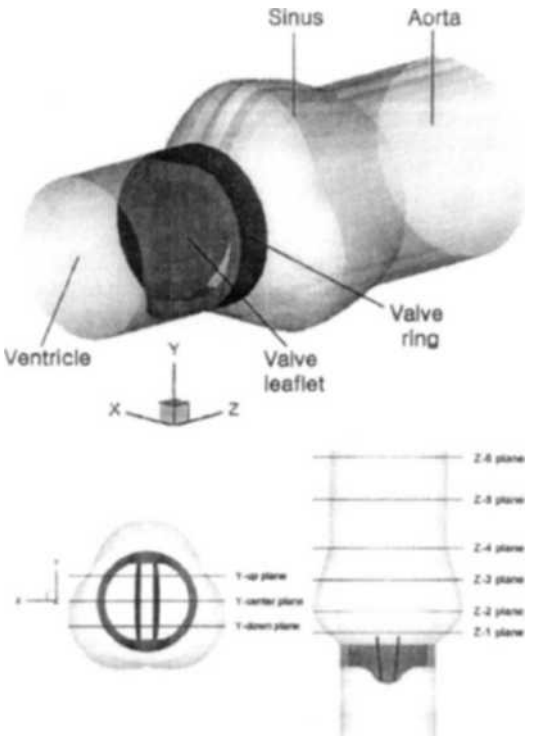

Fig. 2 The valve, sinuses and vessel geometry used for simulation

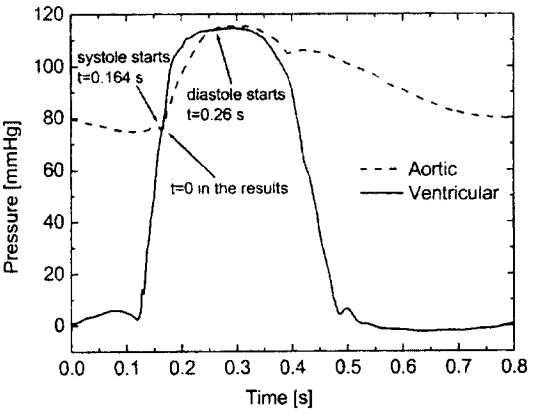

Fig. 3 Thansient ventricular and aortic pressure waveforms at the boundaries in the case 1

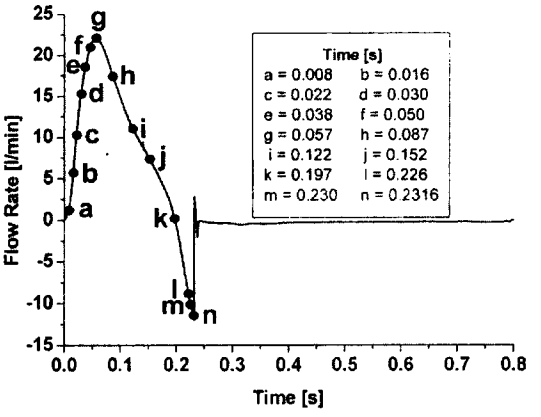

Fig. 4 Transient flow rate of the case 1

For the boundary condition of the case 1, the pressure waveforms, measured in vitro (Thubrikar et al, 1996a ; Thubrikar et al., 1996b)] in the ventricle and the aorta with 75 beats per minute, were used as the pressure boundary conditions for the numerical calculation (Fig. 3). The mass flow wave, resulted from calculation of the case 1 shown in Fig. 4, was employed as a boundary condition in inlet (ventricle) to calculat a the of pulsatile flow of the case 2. In Fig. 4 and below Figures, time t=0 means the beginning of the opening phase of leaflet associated with ventricle contraction (time t=0 in the result figures of present calculation is equal to t=0.164 s in Fig. 3).

Commercial CFD softwares, CFD-ACE+ ver. 6.4 (CFD Research Corporation, USA) and FEMSTRESS (add-on module of CFD-ACE+ ; a finite element structural analysis module), have been adopted to solve the related equations. The current numerical calculation included 68,448 cells. For the case 1, it has taken over 140 hours per one cycle with SMP system (CPU : Alpha EV6.7 667 MHz, Memory : 4 Gbyte) of KISTI Supercomputing Center, KOREA. The calculation time for case 2 has taken about 50 hours with a PC of Intel Pentium III 800 MHz and 512 MB memory.

4. Results and Discussion

4.1 Results of the case 1 (with moving leaflets)

The calculated mass flow wave in the case 1 is shown in Fig. 4. The mass flow wave can be divided into acceleration (a-g), peak systole (g), deceleration (g-k), regurgitation (k-n), and leakage (after n) durations. This mass flow wave has

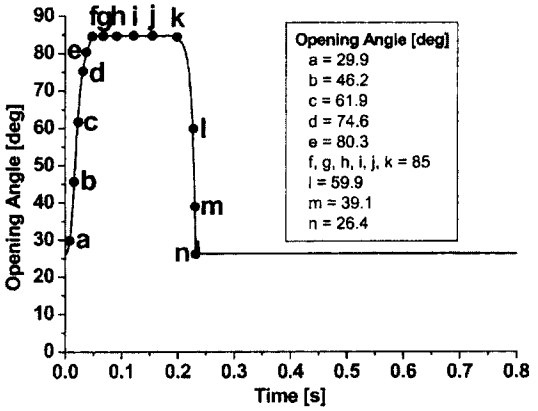

Fig. 5 Transient variation of leaflet opening angle

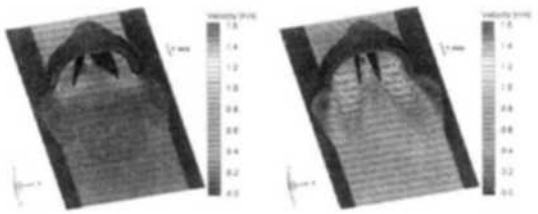

(a) Time position (c) (b) Time position (g)

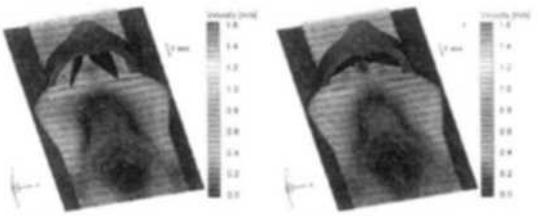

(c) Time position (l) (d) Time position (n)

Fig. 6 Transient velocity vectors of blood flow in Y-center plane

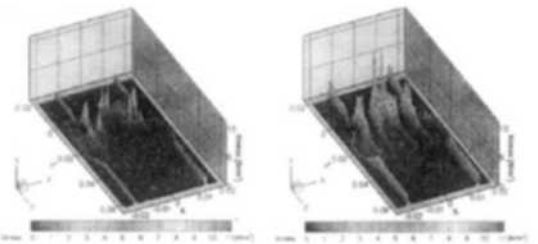

(a) Time position (c) (b) Time position (g)

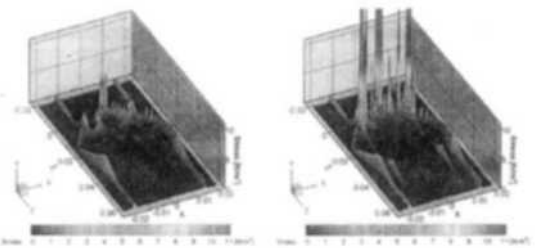

(c) Time position (l) (d) Time position (n)

Fig. 7 Transient shear stress at different time positions

shown a similar tendency to the result measured in the in vitro experiment by Wu et al. (1986).

Transient variation of the leaflet opening angle using the model of interaction between blood flow and leaflet motion is plotted in Fig. 5. Notation used in Fig. 5 matches with that in Fig. 4. The leaflet motion can be divided into five durations; they are rapid opening (a-d), slow opening (d-f), fully opened (f-k), slow closing (k-i), and rapid closing (i-n). The closing velocity of leaflet in the closing phase is about twice faster than that in the opening phase. This trend is also found in the result recorded by a high speed camera (Yuji et al., 2000). When the leaflet starts to contact with the housing (time position (n) in the Fig. 5), rebound of the leaflet takes place because of the inertia effect of leaflet motion and water hammer effect. This phenomenon has been observed in the pulsatile experiment performed in our laboratory.

Velocity vector profiles and shear stress contours in the different time positions at Y-center plane are depicted in Figs. 6 and 7. Notations for time positions can be found in Figs. 4 and 5. Notation (c), (g), (l), and (n) are on the opening phase ($\theta \doteqdot 60°$), on fully opened phase ($\theta = 85°$), on closing phase ($\theta \doteqdot 60°$), and on the right before closure ($\theta = 26.4°$), respectively.

In the opening phase, the blood flows mainly through side orifices between leaflet and housing and the flow rate through center orifice between leaflets is small because of rotational behavior of the leaflets. The fluid emerging from the side orifices flows along the valve leaflets and impinges on the walls of the flow channel. The downstream flow of the valve is shown to be almost uniform. In the fully opened state, three high velocities like jet are found downstream of the valve. The jets from the side orifices are wider and longer than that from the center orifice. The ratio of volumetric flow rate of two side orifice

to that of the center orifice is about 0.785 : 0.215. This seems to suggest that the major part of blood flows through the side orifices, and not the center orifice. Recirculation flow exists in the sinus region and higher velocity regions are found in the upper stream part between the two leaflets. During the closing phase, reversed flow (regurgitation) is formed mainly along the walls in the sinus region and recirculation zones are found in the central region of the sinus. The reverse flow formed along the walls in the sinus region may give effect of washing out valve leaflets, ring, and sinus wall. Generally speaking, flow fields calculated in this study is similar to those visualized by the experiment for pulsatile flow performed by Woo et al. (1986).

Large shear stress regions are found in the vicinity of the valve leaflets, housing, and vessel wall. Especially, in right before the closure of the valve leaflet, shear stress peaks during a short time are shown with about 183 N/m^2 in the vicinity of the front end of leaflets. The higher shear stress is caused by squeeze flow through very narrow gap between the leaflets and the housing.

The extent of red blood cells (RBCs) damage is known to be a function of both the magnitude of shear stress (τ_{xy}) acting on blood corpuscles and their exposure time (t_{exp}) to shear stress fields. An empirical model proposed by Giersiepen et al. (1984) for Hb (Hemoglobin) released by RBCs is as follows;

$$\frac{\Delta Hb}{Hb}(\%) = 3.62 \times 10^{-5} t_{exp}^{0.785} \tau_{xy}^{2.416} \qquad (10)$$

This equation notes that the extent of red blood cell damage depends not only upon the magnitude of shear stress but also upon their exposure time (τ_{exp}) to shear stress fields. Therefore, in view of the red blood cell damage, the shear stress distribution in the fully opened phase is more important, because the exposure time is longer and shear stress is also higher compared to other phases. In the fully opened phase, maximum shear stress found in the vicinity of the front end of leaflets is about 10.7 N/m^2 exemplified by a contour plot in Fig. 7. The distributions of shear stress in Y-top and Y-bottom planes are similar to that of Y-center plane, and the magnitudes of peak shear stress in the two Y planes are smaller than that of Y-center plane.

The calculated flow field cannot be compared in detail to that of experimental result, but the obtained shear stresses are of the same order of magnitude as observed in the experiments of similar in vitro flow problems (Lee et al., 1995; Sakhaeimanesh et al., 1996). Although the peak shear stress value is somewhat different, the distribution characteristics is similar to the results obtained by the two-dimensional CFD analysis using the lattice-Boltzmann methods by M. Krafczyk et al. (2001) and to the results by Choi et al. (2001a, 2001b) using the model introduced in this paper.

According to Giersiepen et al. (1988), the critical shear stress level for the lethal erythrocyte and thrombocyte damage is 200 to 400 N/m^2 for an exposure time of 1 to 10 msec, which is the estimated time for blood cell to pass through heart valve prosthesis. The peak shear stresses calculated in this study are far below the critical shear stress range to cause necrosis of blood cells or lethal erythrocyte and thrombocyte damage.

4.2 Comparison of the case 1 (moving leaflets) and the case 2 (fixed leaflets)

The results of the two approach method are compared; the one is with moving leaflets (case 1, described in section 4.1) and the other is with fixed leaflets (case 2). Figure 8 represent the velocity vectors and shear stress distributions at Y-center plane at the time position (g) at which valve leaflets are fully opened and mass flow rate is in the largest state.

In the case 2 with fixed leaflets, three high velocities like jet are found downstream of the valves and the jets from the side orifices are wider and longer than that from the center orifice. These results show similar tendency to the results of the case 1 with moving leaflets. The ratio of volumetric flow through the two side orifice to that through center orifice is about 0.777 : 0.223, while it is 0.785 : 0.215 in the case 1 with the moving leaflets, which means that these are almost the same in two cases. In the case 1 with

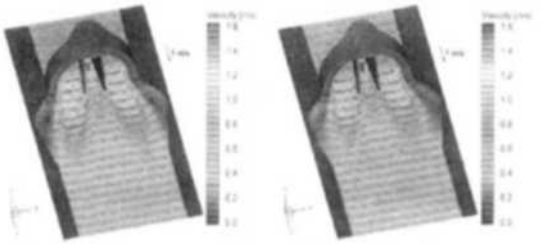

(a) Velocity vector (left : with leaflet motion, right : with fixed leaflet)

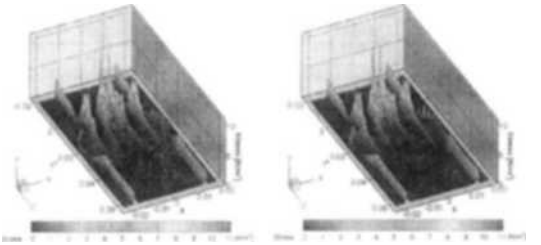

(b) Shear stress (left : with leaflet motion, right : with fixed leaflet)

Fig. 8 Velocity vector and shear stress in Y-center plane at the time position (g)

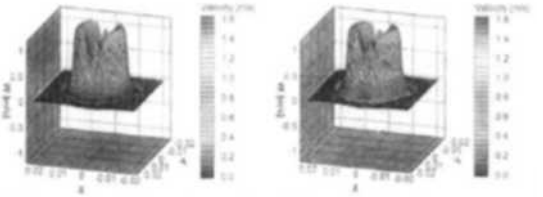

(a) Velocity vector profiles (left : with leaflet motion, right : with fixed leaflet)

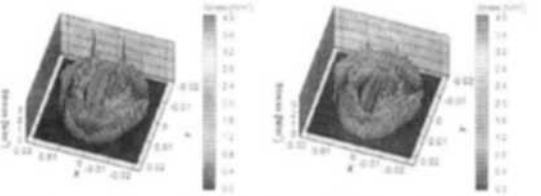

(b) Shear stress distributions (left : with leaflet motion, right : with fixed leaflet)

Fig. 9 Velocity profiles and shear stress contours in Z-1 plane at the time position (g)

the moving leaflets, maximum shear stress found in the vicinity of the front end of leaflets is about 10.7 N/m^2. Maximum shear stress in the case 2 calculated with the fixed leaflets is found to be about 11.3 N/m^2. The velocity and shear stress fields show little difference between two results

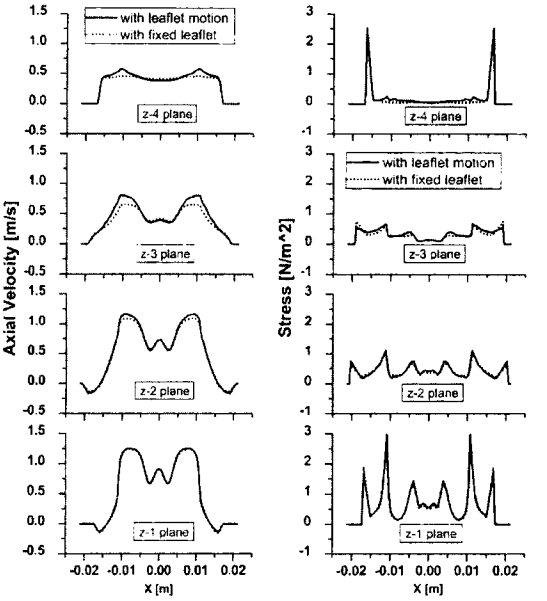

(a) Velocity profile (b) Shear stress profile

Fig. 10 Velocity and shear stress along horizontal center line of Z plane section (time position (g))

with moving leaflets and with fixed leaflet. Axial velocity and shear stress contours in Z-1 plane at the time position (g) are plotted in Fig. 9. It reveals that the flow characteristics obtained by the two approach methods are nearly similar to each other except in a very small region of the flow field.

Velocity and shear stress profiles along the horizontal center line of Z plane sections are plotted in Fig. 10. In right after valve, velocity and shear stress profiles are nearly the same for the two cases. Although a discrepancy between the two approach methods is shown in down-stream, the two approach methods predict the same tendency of the profiles in the view of overall flow field.

5. Conclusions

A transient three-dimensional blood flow interacted with moving leaflets in aorta of a heart is performed using a fluid-structure interaction model introduced in this paper. In this method, a finite volume computational fluid dynamics code

and a finite element structural dynamics code have been used concurrently to solve the flow and structure equations, respectively, since the blood flow and leaflet motion are strongly coupled. The results predict similar tendency compared with the previous experiments.

Also, transient three-dimensional flow with fixed leaflets is calculated for comparison to that with the moving leaflets at the identical flow inlet condition. In a peak systole, the flow fields are nearly similar to that of the case with moving leaflets in general.

Although calculation with fixed leaflets predicts similar flow fields to that of the case with moving leaflets, the analysis including moving leaflets is rigorously required because the simulation with fixed leaflets cannot predict the flow fields during opening and closing phases of the leaflet and also the exposure time to the shear stress fields cannot be exactly determined.

The present research has shown the capability to describe in detail the characteristics of the blood flow and leaflet motion for a complete cardiac cycle, and to overcome the shortness of previous studies where the effect of leaflet motion has been ignored or approximated by simplified assumption. To our knowledge the present study is the first attempt for three-dimensional analysis considering the fluid-structure interaction of moving leaflets associated with a physiological blood flow during a complete heart beat cycle. A fluid-structure interaction model introduced in this paper can be applied to various problems where fluid motion and structure behavior are coupled each other.

Acknowledgment

This study was financially supported by the KOREA RESEARCH FOUNDATION (Project number : KRF-99-042-F00127-F3300).

References

Bluestein, D., Einav, S. and Hwang, N. H., 1994, "A Squeeze Flow Phenomenon at the Closing of a Bileaflet Mechanical Heart Valve Prosthesis," *J. Biomechanics*, Vol. 27, pp. 1369~1378.

Cape, E. G., Yoganathan, A. P. and Levine, R. A., 1990, "A New Theoretical Model for the Non Invasive Quantitation of Mitral Regurgitation," *J. Biomechanics*, Vol. 23, pp. 27~331.

Chandran, J. B., 1985a, "Pulsatile Flow Past a St. Jude Medical Bileaflet Heart," *J. Thorac. Cardiovasc. Surg.*, Vol. 89, p. 743.

Chandran, K. B., Cabel, G. N., Khalighi, B. and Chen, C. J., 1985b, "Laser Anemometer Measurements of Pulsatile Flow Past Aortic Valve Prostheses," *J. Biomechanics*, Vol. 16, No. 10, p. 865.

Choi, C. R. and Kim, C. N., 2001a, "Analysis of Blood Flow Interacted with Leaflets in MHV in View of Fluid-Structure Interaction," *KSME International Journal*, Vol. 15, No. 5, pp. 613~622.

Choi, C. R. and Kim, C. N., 2001b, "Characteristics of Transient Blood Flow in MHVs with Different Maximum Opening Angles Using Fluid-Structure Interaction Method," Korean J. Chem. Eng., Vol. 18, No. 6, pp. 809~815.

Fatermi, R. S. and Chandran, K. B., 1989, "An in Vitro Study of the St. Jude Medical and Edwards Duromedics Bileaflet Valve Using Laser Anemometry," *J. Biomech. Eng.*, Vol. 111, p. 298.

Giersiepen, M., Wurzinger, L. J., Opitz, R. and Reul, H., 1984, "Estimation of Shear Stress Related Blood Damage in Heart Valve Prostheses-in Vitro Comparison of 25 mm Aortic Valves," *International Journal of Artificial Organs*, Vol. 13, No. 5, pp. 300~306.

Giersiepen, M., "Ermittlung Von Stromungsprofilen und Schubspannungen an Herzklappenprothesen Mit Hilfe Der Laser-Doppler-Anemometrie in Pulsatiler Strimung [Thesis]," Aachen : RWTH Aachen, Faculty of Mechanical Engineering.

Gross, J. M., Shermer, C. D. and Hwang, N. H. C., 1988, "Vortex Shedding in Bileaflet Heart Valve Prostheses," *Trans. Am. Soc. Artif. Intern. Organs*, Vol. 34, p. 845.

Hasenkam, J. M., Mygaard, H., Giersiepen, M., Reul, H. and Stodkilde-Jorgensen, H., 1988, "Turbulent Stress Measurements Downstream of

Six Mechanical Aortic Valves in a Pulsatile Flow Model," *J. Biomechanics*, Vol. 21, p. 631.

Krafczyk, M., Cerrolaza, M., Schulz, M. and Rank, E., 1998a, "Analysis of 3D Transient Blood Flow Passing through an Artificial Aortic Valve by Lattice-Boltzmann Methods," *J. Biomechanics*, Vol. 31, p. 453.

Krafczyk, M., Tolke, J., Rank, E. and Schulz, M., 2001b, "Two-dimensional Simulation of Fluid-Structure Interaction Using Lattice-Boltzmann Methods," *Computers and Structures*, Vol. 79, pp. 2031~2037.

Lee, S. C. and Chandran, K. B., 1995, ": Numerical Simulation of Instantaneos Bakflow through through Central Clearance of ···," *Med. Bio. Eng. Comp.*, Vol. 33, p. 257.

Nygaard, H., Paulsen, P. K., Hasenkan, J. M., Pedersen, E. M. and Rovsing, 1994, "Turbulent Stresses Downstream of Three Mechanical Aortic Valve Prostheses in Human Beings," *J. Thorac. Cardiovas. Surg.*, Vol. 107, p. 438.

Reul, H., Vahlbruch, A., Giersiepen, M, Schmitz-Rode, T. H., Hirtz, V., Effert, S., 1990, "The Geometry of the Aortic Root in Health, at Valve Disease and After Valve Replacement," *J. Biomechanics*, Vol. 23, No. 2. pp. 181~191.

Sakhaeimanesh, A. A., Morsi, Y., Tansley, G., 1996, *Proc. 10th Conf. Eur. Soc. Biomech.*, Leuven, Belgium.

Thubrikar, M. J., Selim, G, Robicsek, F. and Fowler, B, 1996a, "Effect of the Sinus Geometry on the Dynamics of Bioprosthetic Heart Valves (abstract)," *Ann. Biomed. Eng.*, Vol. 24, S3.

Thubrikar, M. J., Selim, G., Robicsek, F. and Fowler, B., 1996b, "Effect of the Sinus Geometry on the Dynamics of Bioprosthetic Heart Valves (abstract)," *Proceedings of the 18th Annual International Conference of the IEEE Engineering in Medicine and Biology Society Amsterdam*, The Netherlands, pg. 10, November.

Woo, Y. R. and Yoganathan, A. P., 1986, "Pulsatile Flow Velocity and Shear Stress Measurements in the St. JudeValve Prosthesis," *Scandinavian Journal of Thoracic and Cardiovascular Surgery*, Vol. 20, pp. 15~28.

Woo, Y. R. and Yoganathan, A. P., 1986, "Pulsatile Flow Velocity and Shear Stress Measurements on the St. Jude Valve Prosthesis," *Scand. J. Thorac. Cardiovasc. Surg.*, Vol. 20, p. 15.

Wu, Z. J. and Hwang, H. C., 1995, "Ventricular Pressure Slope and Bileaflet Mechanical Heart Valve Closure," *ASAIO Journal*, Vol 41, pp. M763-M767.

Yang, H. Q. and Makhijani, V. B., 1994, "A Strongly Coupled Pressure-Based CFD Algroithm for Fluid-Structure Interaction," *Proceeding of 32nd Aerospace Sciences Meeting and Exhibit*, Reno, NV, AIAA-94-0719.

Yuji, O., Yukiaki, K., Tishiyuki, S., Yoshinoti, M., Toshio, Y. and Takeyoshi, D., 2000, "Effect of the Sinus of Valsalva on the Closing Motion of Bileaflet Prosthetic Heart Valves," *Artif. Organs*, Vol. 24, No. 4, pp. 308~312.